ACS OMEGA

http://pubs.acs.org/journal/acsodf

Article

# Multilayer Transparent Wood with Log Color Composed of Different Tree Species

Jichun Zhou, Yajing Wang, Jing Wang, and Yan Wu*

Cite This: *ACS Omega* 2022, 7, 46303−46310

Read Online

ACCESS | Metrics & More | Article Recommendations

**ABSTRACT:** In this experiment, a multilayer transparent wood with different surface and core layers of tree species was prepared, which has log color. The purpose is to explore the feasibility of preparing multilayer transparent wood from different tree species as raw materials. The experiment first removed partial lignin from the veneers to obtain the wood templates. Then, tree species with rich texture and color as the surface layer wood and tree species with less texture as the core and bottom wood were selected. Finally, the resin-impregnated wood templates were laminated and dried to obtain samples. The results show that wood fiber and resin have good coordination, and the laminated structure is conducive to weakening the anisotropy of transparent wood. Transparent wood has better mechanical property and hydrophobicity than original wood. The above shows that this transparent wood has a large elastic mechanism for the selection of tree species, and the thickness optics can be adjusted according to tree species and wood layers. It has good application prospects in interior decoration or as outdoor structural material.

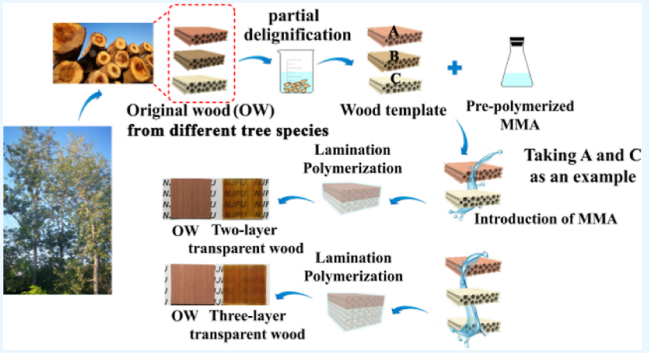


## 1. INTRODUCTION

Research studies have shown that transparent wood has high light transmittance, low thermal conductivity, excellent mechanical properties, and the raw materials used were easy to degrade.[1,2] In recent years, the research field of transparent wood has been continuously expanded. In addition to focusing on photoelectric equipment, flexible devices, green buildings, and so forth[3] people have gradually carried out research on transparent wood as a functional biocomposite for daily home furnishing. In 2020, Fu et al.[4] made transparent wood films emit isotropic, homogeneous, and soft light by introducing CdSe/ZnS quantum dots into the wood templates. The samples were then densified and coated with cetyltrimethoxysilane to impart hydrophobicity. The prepared samples can be used in interior design, such as the laminated cover panels of furniture and the shells of lamps. In the same year, Mi et al. (2020) obtained textured transparent wood, which has low thermal conductivity, good UV blocking ability, and excellent mechanical properties, with toughness up to 2.73 MJ $m^{-3}$ and tensile strength of 91.95 MPa.[5] It can be applied to indoor panels, transparent windows, conceptual transparent roofs, and so forth. The above shows that transparent wood has broad application prospects as structural or decorative materials.

Transparent wood can change the hydrophilicity, opacity, low conductivity, wet expansion, and dry shrinkage of logs to a certain extent. Therefore, as a new achievement of wood modification, it has attracted people's attention. At the same time, for transparent wood itself, people are constantly optimizing its preparation process and improving its performance. For example, thin transparent veneer is highly anisotropic and the material is not homogeneous enough. In addition, in order to maintain good light transmittance of the sample, the increase of its thickness is limited. To solve the above problems, the concept of transparent plywood was first proposed by Fu et al.[6] By adjusting the volume fraction of cellulose and the lamination angle between wood, transparent plywood with different mechanical properties and light transmittance can be obtained. The results showed that regardless of the lamination angle being orthogonal or quasi-isotropic, the ultimate transverse (perpendicular to the wood grain direction of the specimen surface) tensile strength and elastic modulus of the multilayer transparent plywood were significantly higher than those of the single-layer transparent plywood due to the lamination design. Moreover, single-layer transparent veneer has high anisotropy, which is significantly weakened by multilayer transparent plywood. At present, most

Received: July 31, 2022
Accepted: November 17, 2022
Published: December 6, 2022

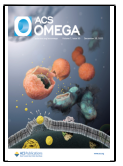

ACS Publications

© 2022 The Authors. Published by American Chemical Society

studies believe that multilayer transparent wood has more advantages than single-layer transparent wood in optical and mechanical properties.[7−9]

In fact, through reading the literature,[10−12] it can be seen that compared with the staggered direction lamination, same direction lamination can also reduce the anisotropy of transparent wood (only the reduction effect is slightly lower than that of the staggered lamination), and the light transmittance of the sample is better. Therefore, the laminated structures used in this paper are all laminated in the same direction along the wood fibers. At present, there is little research on the same sample prepared by different tree species. In order to expand the selection range of transparent wood for raw material tree species, this experiment prepared a multilayer transparent wood with different tree species in the surface and core layers, and no additional adhesive was used in the lamination process. In addition, because lignin or other chromophoric groups are completely removed, the previous transparent wood is colorless and textureless. On the basis of lacking the esthetic and tactile characteristics of natural wood itself, the mechanical strength of wood formwork will also be reduced. Therefore, this paper prepared esthetic transparent wood with wood texture and color by retaining partial lignin. Moreover, such multilayer transparent wood has different laminated numbers (two or three layers), so as to explore the effects of tree species differences and wood lamination number on the properties of multilayer transparent wood. In the pre-experiment, our team explored the optimal process parameters for acid delignification,[13] and the specific parameters and methods are described in detail in the experimental section of this paper. In the experiment, the representative tree species of softwood and hardwood were selected: Chinese fir, *Betula alnoides*, and basswood. This study broadens the selection range of tree species for transparent wood preparation, saves costs, and effectively responds to the long-term challenge of preparing transparent thick wood and reducing the anisotropy of transparent wood, so as to continuously tap the application potential of this multilayer transparent wood as new home materials.

## 2. EXPERIMENTAL PART

**2.1. Experimental Materials.** Chinese fir (*Cunninghamia konishiiHayata*), *B. alnoides* (*Betula*), and basswood (*Tilia*) are veneers used in the production line of furniture factory, and they are all from Yihua Lifestyle Technology Co., Ltd., China. The samples are obtained by wood rotary cutting, which are chord sections. In the experiment, the samples were processed to 20 mm (length) × 20 mm (width) × 0.5 mm (thickness). The air-dry density relative, moisture content, and thickness of the tree species are shown in Table 1. Bout experimental chemical reagent: absolute ethanol ($C_2H_6O$), glacial acetic acid ($CH_3COOH$), and sodium hydroxide (NaOH) were obtained from Nanjing Chemical Reagent Co., Ltd. Sodium chlorite ($NaClO_2$) was purchased from Shanghai Macklin Biochemical Co., Ltd. Methyl methacrylate (MMA) was supplied by Shanghai Aladdin Biochemical Technology Co., Ltd. Azobisisobutyronitrile (AIBN) was obtained from Tianjin Benchmark Chemical Reagent Co., Ltd.

**Table 1. Air-Dry Density Relative, Moisture Content, and Thickness of the Tree Species**

| tree species | air-dry density relative ($g/cm^3$) | moisture content (%) | thickness (mm) |
|---|---|---|---|
| Chinese fir (A) | 0.39 | 11.24 | 0.50 |
| *B. alnoides* (B) | 0.64 | 9.71 | 0.50 |
| basswood (C) | 0.42 | 8.66 | 0.50 |

**2.2. Experimental Procedure.** The transparent wood is prepared by impregnating delignified wood template with a refractive-index-matched resin. The laminated structure is parallel and codirectional along the wood fibers.

*2.2.1. Preparation of Wood Templates.* Chinese fir, *B. alnoides*, and basswood were dried at 103 °C for 6 h to constant weight and then stored in a desiccator for later use. The experiment used the chlorite method to remove partial lignin, and the optimized process parameters were as follows: the concentration of $NaClO_2$ was 1 wt %, the reaction time was 1.5 h, and the reaction temperature was 90 °C. Then, the wood templates were taken out and washed with deionized water for 2−3 times. Afterward, the wood templates were placed in absolute ethanol for use to isolate air and moisture. In order to facilitate the analysis and elaboration of this paper, the original wood of Chinese fir is called OW-A for short, and the corresponding wood template is called FW-A for short, and so on, the original wood of *B. alnoides* is called OW-B and the corresponding wood template is called FW-B for short, and the original wood of basswood is referred to as OW-C and the corresponding wood template is referred to as FW-C.

*2.2.2. Preparation of Pre-polymerized MMA.* NaOH solution was used to remove the polymerization inhibitor in the monomer MMA solution by liquid separation. Then, 0.35−0.40 wt % AIBN was added to the MMA solution as the initiator. After that, MMA solution was heated in a water bath at 75 °C for 15 min. When the time was up, the solution (pre-polymerized MMA) was taken out immediately and immersed into an ice−water bath to cool to room temperature for later use.

*2.2.3. Acquisition of Multilayer Transparent Wood.* All the wood templates were immersed in the pre-polymerized MMA solution, and the samples were allowed to stand under vacuum for about 1 h. Afterward, Chinese fir or *B. alnoides* with rich texture and color under partial delignification as the surface layer wood and basswood with less texture as the core layer and bottom layer wood were selected. Subsequently, the wood templates of the corresponding layers were laminated according to the wood texture direction. After that, they were clamped and fixed in the mold, sealed, and wrapped with tinfoil and then heated and polymerized in the oven at 70 °C for 5 h. Finally, different kinds of multilayer transparent wood were obtained. The samples consist of two-layer transparent wood and three-layer transparent wood, as shown in Figure 1. In the two-layer transparent wood, Chinese fir is the surface layer and basswood is the bottom layer, which is called TW-AC; *B. alnoides* is the surface layer and basswood is the bottom layer, which is called TW-BC. Among the three-layer transparent wood, Chinese fir is the surface layer, basswood is the core lay and bottom layer, which is called TW-ACC; and *B. alnoides* is the surface layer, basswood is the core lay and bottom layer, which is called TW-BCC. In order to facilitate the subsequent analysis in the article, the following abbreviations are used. TW-AC and TW-BC are both 20 mm (length) × 20 mm (width) × 1.15 mm (thickness). TW-


https://doi.org/10.1021/acsomega.2c04842
ACS Omega 2022, 7, 46303−46310

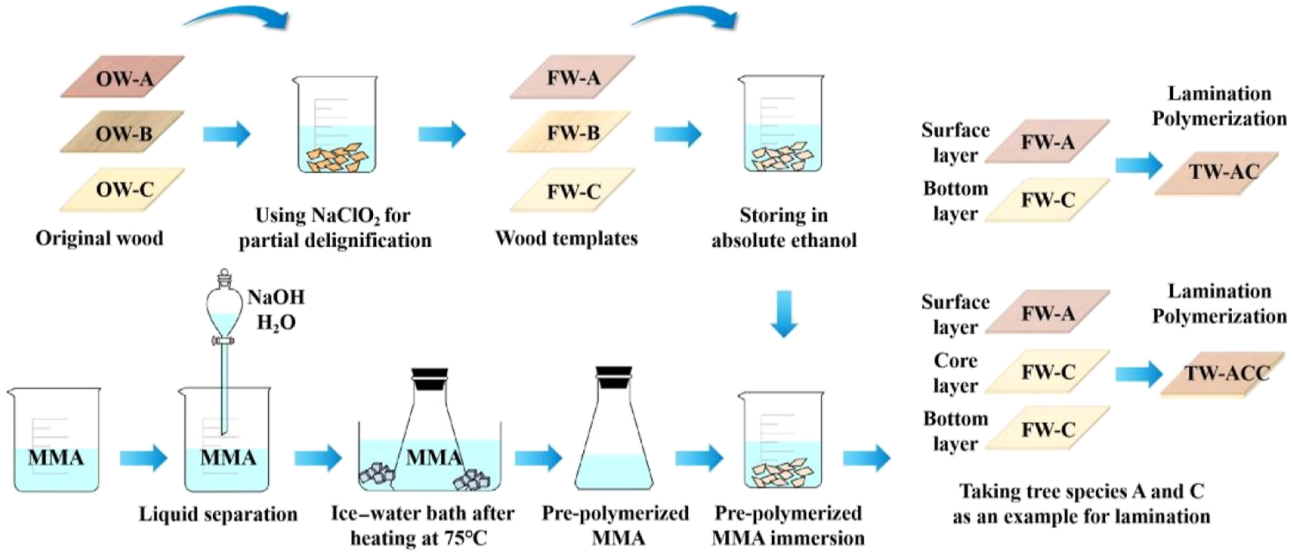


**Figure 1.** General flowchart of multilayer transparent wood.

ACC and TW-BCC are both 20 mm (length) × 20 mm (width) × 1.60 mm (thickness).

## 3. TEST SECTION

**3.1. Chemical Component Test.** The National Renewable Energy Laboratory (NREL) method was used to test the contents of three major elements (lignin, cellulose, and hemicellulose) of the original wood and wood templates.

In addition, infrared spectrometer (BRUKER-ALPHAII 12528039) was used to test OW-A, OW-B, OW-C, TW-AC, TW-ACC, TW-BC, and TW-BCC and obtain the corresponding infrared spectrograms. By marking the characteristic absorption peaks of the infrared spectrum, the chemical composition of the samples can be qualitatively analyzed.

**3.2. Color Difference and Gloss Test.** Both the color difference test and gloss test are non-destructive tests and are aimed at the physical properties of the sample surface. Therefore, the difference of the multilayer transparent wood core layer has no effect on the numerical test, so TW-AC and TW-ACC can be regarded as a type of samples in this test. The color difference meter (PANTONE) and gloss meter (HG268, SN: H680029) were used here to test the color difference and gloss of the OW-A, OW-B and TW-AC, TW-BC. It should be noted that for the color difference test because the original wood and transparent wood have textures, five points were randomly measured for dark color part and five points for light color part and then the average values were taken.

**3.3. Optical Characteristic Test.** The light transmittance and haze of the samples OW-A, OW-B, OW-C, TW-AC, TW-ACC, TW-BC, and TW-BCC under 350−800 nm wavelength light was measured using a UV spectrophotometer. The calculation formula of haze is as follows, which follows the standard of ISO-14782.

$$\text{Haze} = [(\tau 4/\tau 2) - (\tau 3/\tau 1)] \times 100 \quad (1)$$

where $\tau 1$ is the beam of incoming light, $\tau 2$ is the beam of transmitted light passing through the sample, $\tau 3$ is the beam of diffused light from the system, and $\tau 4$ is the beam of diffused light from the system and samples.

**3.4. Hardness Test.** The Shore hardness tester LX-D was used to measure hardness of OW-A, OW-B, OW-C, FW-A, FW-B, FW-C, TW-AC, TW-ACC, TW-BC, and TW-BCC. This instrument implemented the JB6148-92 standard. It should be noted that the next test point should be at least 6 mm away from the previous one.

**3.5. Electron Microscope Test.** An FEI Quanta 200 scanning electron microscope was used to observe the micromorphology of OW, FW, and TW. Mainly, the cross section and longitudinal section of the samples were observed.

**3.6. Water Resistance Test.** According to GB/T1934.1-2009, the samples OW-AC, OW-ACC, OW-BC, OW-BCC, TW-AC, TW-ACC, TW-BC, and TW-BCC were placed into the oven at 60 °C for 4 h to dry and weigh ($m_o$). Next, the samples were immersed in distilled water and, pressed at least 50 mm below the water surface with a metal mesh, keeping the water temperature within the range of 18−22 °C. Then, the samples placed in the water were weighed for the first time after 6 h and then weighed once after 24, 48, 96, and 192 h, respectively, until the difference between the last two moisture contents was less than 5% and the maximum water absorption rate was considered to have been achieved. The formula for calculating water absorption is as follows.

$$A\ (\%) = (m - m_o)/m_o \times 100 \quad (2)$$

where $A$ is the water absorption and $m$ (g) is the mass of the sample after water absorption.

At the same time, the original wood and multilayer transparent wood were placed on the stage, respectively, and 2 $\mu$L of deionized water was dropped on the sample surface to observe the whole process of water droplet contacting the sample surface until the diffusion and record the contact angle of water droplets on the sample surface at the 50th second.

**3.7. Mechanical Performance Test.** The universal mechanical testing machine (SANS-CMT6104) was used to stretch the samples (along the wood fiber direction and perpendicular to the wood fiber direction, respectively). The sample was first fixed between the upper and lower fixtures. Then, the lower fixture was fixed, and the upper fixture moved vertically upward at 3 mm/min until the sample was stretched to fracture. The mechanical value $F$ at the fracture point of the sample was recorded. Subsequently, the tensile strength of the sample was calculated.



https://doi.org/10.1021/acsomega.2c04842
ACS Omega 2022, 7, 46303−46310

Table 2. Three Elements of Original Wood and Wood Templates

| tree species | Chinese fir | | *B. alnoides* | | basswood | |
|---|---|---|---|---|---|---|
| name | OW-A | FW-A | OW-B | FW-B | OW-C | FW-C |
| lignin/% | 34.58 | 24.78 | 34.25 | 23.65 | 23.01 | 16.53 |
| cellulose/% | 33.31 | 32.31 | 42.25 | 41.33 | 42.50 | 41.52 |
| hemicellulose/% | 17.40 | 15.83 | 20.23 | 18.73 | 23.58 | 22.80 |

$$\sigma(\mathrm{MPa}) = F(\mathrm{N})/S(\mathrm{mm}^2) \quad (3)$$

where $S$ is the initial cross-sectional area of the sample along the tensile direction.[14]

## 4. RESULTS AND DISCUSSION

**4.1. Wood Component Analysis.** Lignin, as a very complex natural polymer, strongly absorbs light at the visible wavelength of 380−780 nm, and hemicellulose and cellulose are colorless in optics.[15,16] Here, it can be seen from Table 2 that after partial delignification, the cellulose and hemicellulose contents of the tree species only slightly decreased. For Chinese fir, *B. alnoides,* and basswood, the lignin content decreased by 28.34, 30.95, and 28.29%, respectively. Here, partial lignin is removed from the original wood so that the resin can be more fully impregnated into the lumen of the wood. The reason for not removing all the lignin is to save energy consumption and reduce experimental time and chemicals; on the other hand, because part lignin is retained, the wood templates are not so fragile and are not significantly decolorized. The correspondingly produced transparent wood can have the texture and color of solid wood on the basis of light transmission. It should be noted that for low-density tree species, complete delignification will make the wood template fragile, which is not conducive to the production of large format transparent wood.[17] The preparation method of this experiment can effectively avoid this problem.

Figure 2 shows the infrared absorption spectrograms of the original wood and multilayer transparent wood. The samples

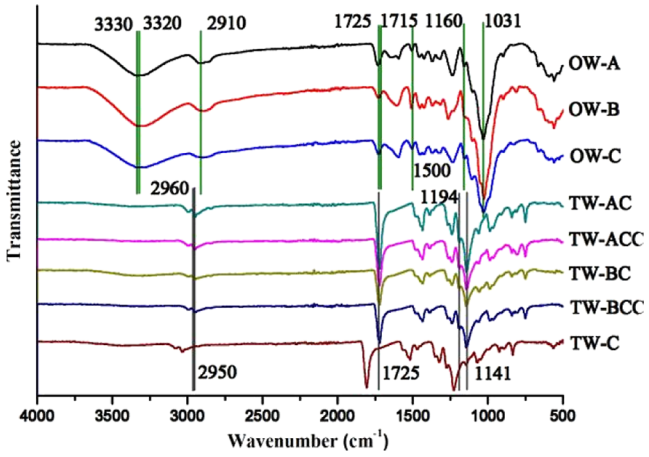


**Figure 2.** Infrared spectrogram of OW-A, OW-B, OW-C, TW-AC, TW-ACC, TW-BC, and TW-BCC.

OW-A, OW-B, and OW-C are timbers with similar main components. The peak positions marked in the spectrum show the main functional groups of cellulose (C−O−C and −OH) stretching vibration at 1160 and 3320 $cm^{-1}$, respectively; the main functional groups of lignin (−OH, −C═O, and aromatic ring skeleton groups) stretching vibration at 3320, 1725, and 1500 $cm^{-1}$, respectively, including methoxy group stretching vibration at 1031 and 2910 $cm^{-1}$; hemicellulose acetyl group stretching vibration at 1715, and phenolic compounds in the extract stretching vibration at 3300 $cm^{-1}$.[18] The test shows that the samples TW-AC, TW-ACC, TW-BC, and TW-BCC add the characteristic peaks of the resin PMMA (the chemical formula of PMMA is $C_5H_8O_2$) on the basis of retaining part of the characteristic peaks of the wood: 1194 and 1141 $cm^{-1}$ are the characteristic peaks of C−O, 1725 $cm^{-1}$ is the characteristic peak of C═O, and 2960 and 2950 $cm^{-1}$ are the characteristic peaks of C−H.[19] It can be seen that although the tree species in the surface layer and core layer of multilayer transparent wood are different, the samples all have the same rule, that is, PMMA has successfully impregnated the wood template and has a good synergy with it.

**4.2. Color Difference and Gloss Analysis.** Through reading books, we know that the visual physical quantities composed of color parameters and gloss parameters are closely related to people's psychology,[20] so this article tested the following two physical parameters. As shown in Figure 3a,b, compared with the lightness value L of OW-A and OW-B, the lightness value L of TW-AC and TW-BC increased by 10.79 and 13.44%, respectively, due to the filling of transparent resin PMMA, while the higher L value of the wood template was due to the slight bleaching of wood by sodium chlorite. In the test parameters, the *a* value represents the degree of red-green, the *b* value represents the degree of yellow-blue; positive value is more red or yellow, and negative value is more green or blue. The higher the absolute value is, the darker the color is.[21] Regarding the *a* and *b* values of Chinese fir and *B. alnoides*, from veneer to wood templates and then to the transparent wood, there is a trend of first decline and then increase, and the *a* and *b* values of the finished samples are both higher than the original samples, which indicates that the transparent wood in this experiment retained most of the texture and color of the solid wood. Lignin is the main chromogenic component in wood. From the color difference test, it can also be seen that the wood template retains part of the lignin because the *b* value of FW is only slightly lower than that of OW (the higher the lignin content is, the more yellowish the sample is, and the higher *b* value is). In terms of chromaticity, most of the surface texture colors of wood are in the orange-yellow color system, showing the warm color, which is an important reason why wood can give people a warm visual sense and is widely popular. Therefore, the esthetic transparent wood with wood color and texture prepared in this experiment is in line with ergonomics and can give people a good feeling.

The gloss value is determined by the specular reflection ability of the sample surface, and there is a positive correlation between them.[20] As shown in Figure 3c, it can be seen that there is a significant difference in the gloss between the original wood and transparent wood. Because of the resin in the transparent wood effectively filling the wood template, the unevenness of the original wood surface is reduced, and the specular reflection of the wood to the light is increased, so the


https://doi.org/10.1021/acsomega.2c04842
ACS Omega 2022, 7, 46303−46310

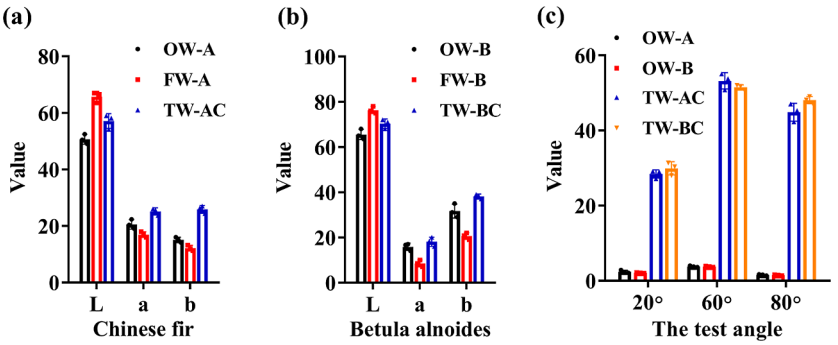


**Figure 3.** Surface properties of samples. (a) Color difference of OW-A, FW-A, and TW-AC. (b) Color difference of OW-B, FW-B, and TW-BC. (c) Gloss of OW-A, OW-B, TW-AC, and TW-BC.

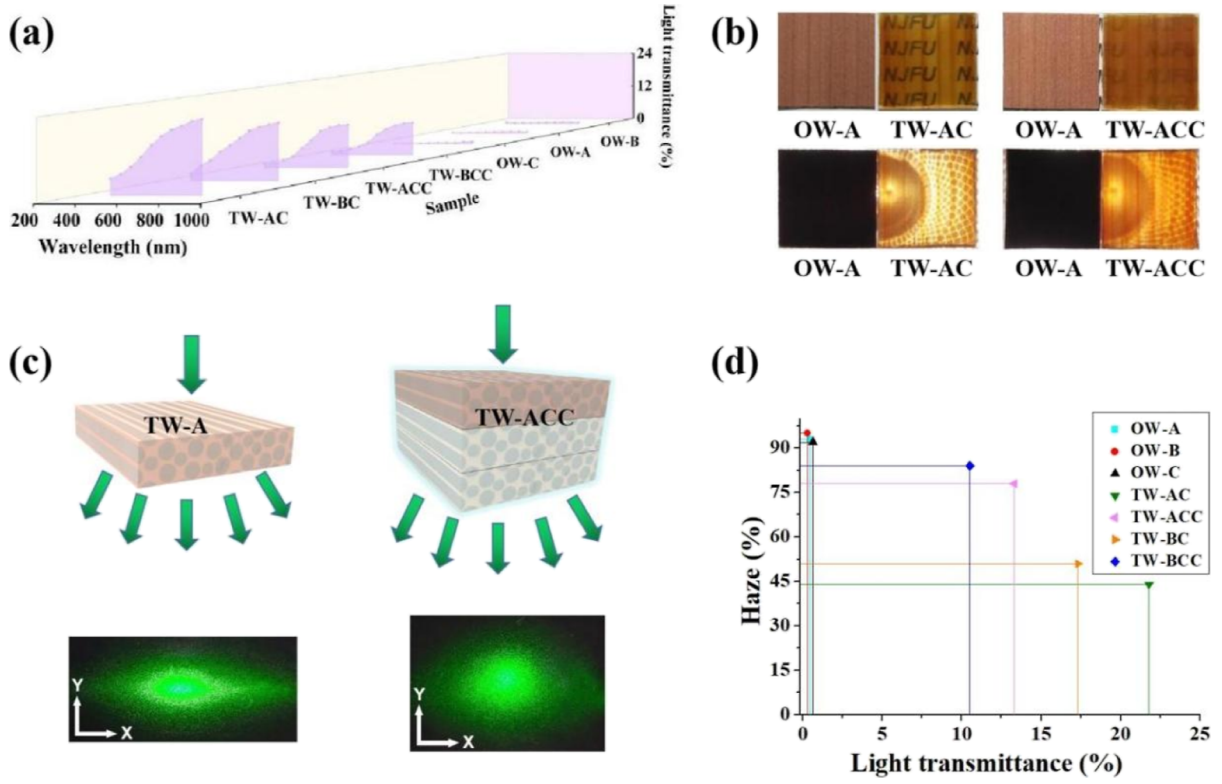


**Figure 4.** Optical characteristic of samples. (a) Light transmittance of OW-A, OW-B, OW-C, TW-AC, TW-ACC, TW-BC, and TW-BCC. (b) Photos of OW-A, TW-AC, and TW-ACC under sunlight and specific light source. (c) Laser scattering image of TW-A and TW-ACC. (d) Light transmittance values and corresponding haze values of various types of samples at a wavelength of 800 nm.

gloss of the samples is improved. According to the literature, the reflectivity that the human eye feels comfortable with is 40−60%. Combined with the values as shown in Figure 3c, it is concluded that the multilayer transparent wood is suitable for using as the material in daily life. Although two kinds of multilayer transparent wood TW-AC and TW-BC have different tree species of surface layers, the gloss of the two is similar. It can be concluded that the effect of resin filling polymerization on the micropores of wood is consistent.

**4.3. Optical Characteristic Analysis.** Figure 4a,d shows the light transmittance and haze of the samples. Regarding the multilayer transparent wood laminated with Chinese fir and basswood, the light transmittance of TW-AC is 21.33% higher than that of OW-A and the light transmittance of TW-ACC is 12.82% higher than that of OW-A; in terms of the multilayer transparent wood laminated with *B. alnoides* and basswood, the light transmittance of TW-BC is increased by 17.01% compared with OW-B and the light transmittance of TW-BCC is increased by 10.21% compared with OW-B. It can be seen that with the increase of the number of wood layers, the light transmittance of transparent wood decreases and the haze increases, which are negatively correlated. Moreover, the increase of the number of sample layers weakens the anisotropy of transparent wood and makes the material more homogeneous. Figure 4c shows that TW-A and TW-ACC are irradiated by a beam of laser, respectively. Compared with single-layer transparent wood, multilayer transparent wood reduces the difference of light scattering in *X* and *Y* directions. According to the author's analysis, this is because TW-ACC is not only filled with resin in wood tracheids but also has a thin resin layer between layers. The resin layer is an isotropic material. Therefore, even if the sample was laminated in the same direction, it can reduce the anisotropy of light scattering. The phenomenon and mechanism of light scattering by TW-B


https://doi.org/10.1021/acsomega.2c04842
ACS Omega 2022, 7, 46303−46310

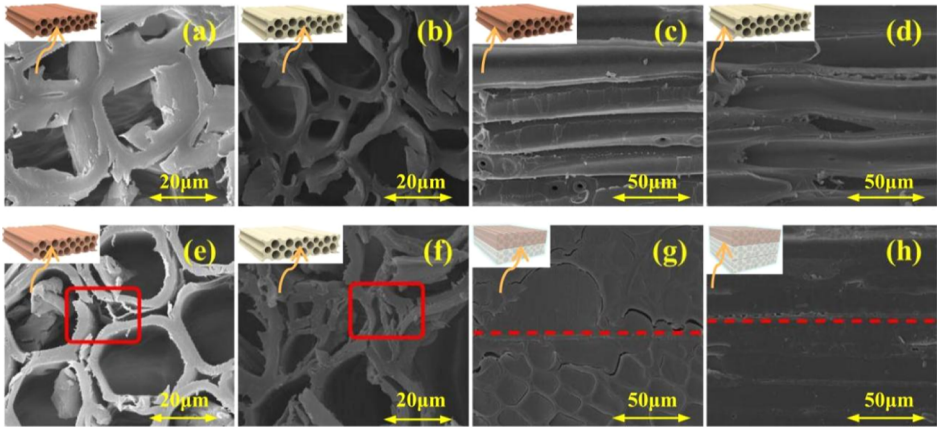


**Figure 5.** SEM images of samples. (a) Cross section of OW-A. (b) Cross section of OW-C. (c) Longitudinal section of OW-A. (d) Longitudinal section of OW-C. (e) Cross section of FW-A. (f) Cross section of FW-C. (g) Cross section of TW-AC. (h) Longitudinal section of TW-ACC.

and TW-BCC are the same as TW-A and TW-ACC. Here, the transparent wood has rich color and texture, especially under the illumination of the specific light source, which has more esthetic characteristics. Some samples are shown in Figure 4b, which were taken under sunlight and the specific light source, respectively. It should be added that due to the specific light source set in the dark environment, the original sample OW-A appears black as shown in Figure 4b due to its opacity.

**4.4. Hardness Analysis.** According to the test, the results show that the hardness values of OW-A, OW-B, and OW-C are 67, 71, and 70HD, respectively; the hardness values of the multilayer transparent wood TW-AC, TW-ACC, TW-BC, and TW-BCC are 77, 78, 82, and 82HD, respectively (the higher the value, the greater the hardness). The hardness values of the multilayer transparent wood are significantly increased by 9.86−15.49% compared with the original wood. This is because the hardness value of the cured PMMA itself is higher than that of the wood, and when PMMA is immersed in the wood templates and polymerized successfully, the hardness values of the modified wood are increased. In addition, the bottom layer wood of multilayer transparent wood was tested: the material is modified wood TW-C and its hardness value is also increased by 14.29% compared with the original OW-C. It can be seen that the material of multilayer transparent wood is hard and wear-resistant, which is suitable for use as daily furniture materials.

**4.5. Electron Microscope Analysis.** Figure 5a−h shows the micro-topography of the samples. Figure 5a is the cross section of OW-A. It can be seen that Chinese fir, as the coniferous wood, is mainly composed of tracheids with small diameter, thick wall, and neat and uniform arrangement; Figure 5b is the cross section of OW-C. In Figure 5b, the pore size is different, the whole cell wall is thin, and the cavity is large. Figure 5c,d shows the longitudinal sections of OW-A and OW-C, respectively. Figures 5e and 6f show the cross sections of wood templates. It can be found that the cell walls of FW-A and FW-C become thinner as a whole, and there are obvious pores in the intercellular layer and the middle layer of the secondary wall $S_2$. This corresponds to the calculation of the above three major elements, indicating that part of the lignin in the wood has been removed, but the overall structure has not been destroyed.[22] Figures 5g and 6h, respectively, present the local characteristics of TW-AC and TW-ACC. The above illustrates that the resin PMMA fully impregnates and fills the wood tracheid and parts lacking lignin. The red line in Figure 5h is a thin resin layer, with basswood on the top and Chinese fir on the bottom. This shows from the side that transparent wood can reduce the anisotropy of the original wood and make the material more homogeneous. It can be seen that different tree species can be effectively laminated through the penetration and cross-linking of impregnated resin. The disadvantage is that the bonding interface between PMMA and wood is not fully bonded, and there are still a small number of pores. This is one of the reasons why the light transmittance of multilayer transparent wood still needs to be improved.

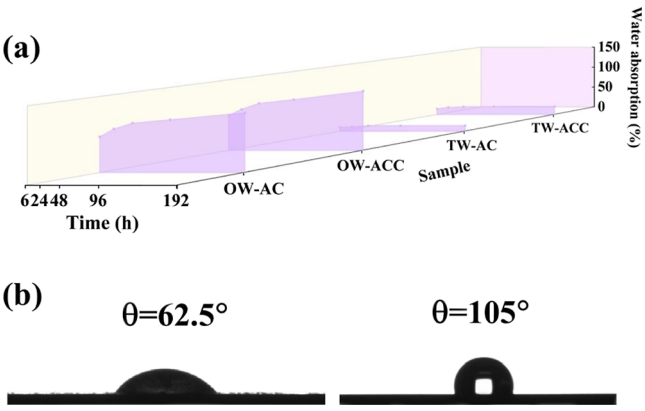


**Figure 6.** Water resistance of samples. (a) Water absorption of OW-AC, OW-ACC, TW-AC, and TW-ACC. (b) Water contact angle of the original wood and multilayer transparent wood.

**4.6. Water Resistance Analysis.** The water absorption of the original wood and multilayer transparent wood is shown in Figure 6a. Here, take the multilayer wood laminated with Chinese fir and basswood as an example for analysis. It can be seen that the water absorption of OW-AC and OW-ACC is significantly higher than that of transparent wood TW-AC and TW-ACC. The reason why the original wood has the disadvantage of wet expansion and dry shrinkage is that it has a unique three-dimensional porous structure formed by natural growth, especially in the humid environment, it is easy to absorb a lot of water.[23] However, after the resin has effectively and fully impregnated the wood templates, the original porous structure is basically eliminated, and the overall structure of multilayer transparent wood becomes more homogenized and densified compared with the original


https://doi.org/10.1021/acsomega.2c04842
ACS Omega 2022, 7, 46303−46310

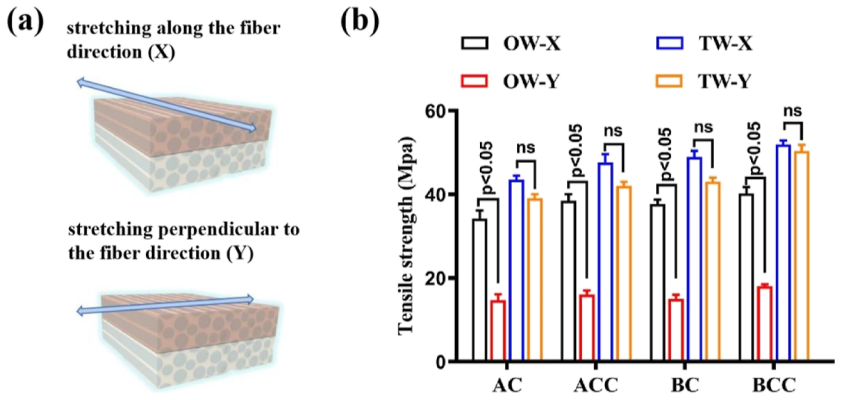


**Figure 7.** Mechanical performance of the samples. (a) Model diagram of stretching along the fiber and perpendicular to the fiber. (b) Tensile strength of OW-AC, TW-AC, OW-ACC, TW-ACC, OW-BC, TW-BC, OW-BCC, and TW-BCC.

wood. In addition, the resin PMMA has hydrophobic groups. As shown in Figure 6b, these are the images at the 50th second when the droplet contacted the sample. The water contact angle of the original wood is 62.5°, showing hydrophilicity; the water contact angle of the modified transparent wood is up to 105°, which has good hydrophobicity. The water contact angle of original wood decreased slightly with the increase of time, and the water contact angle of transparent wood was always stable. Therefore, the weight gain rate of transparent wood after water absorption is significantly lower than that of original wood, and its water resistance is better, so it also has better dimensional stability.

**4.7. Mechanical Performance Analysis.** The tensile strength of each type of samples is shown in Figure 7. The results show that for the transparent wood laminated with Chinese fir and basswood, the tensile strength along the grain direction of TW-AC is increased by 27.26% compared with that of OW-AC, and TW-ACC is increased by 24.86% compared with OW-ACC; for the transparent wood laminated with *B. alnoides* and basswood, the tensile strength along the grain direction of TW-BC is 30.50% higher than that of OW-BC, and TW-BCC is 27.98% higher than OW-BCC. Combined with the mechanical strength perpendicular to the grain direction, OW shows high anisotropy of thin wood, whereas multilayer transparent wood reduces the difference of mechanical values in the two tensile directions. The thin resin layer between wood layers is an isotropic high-strength material. Therefore, even if transparent wood is laminated in the same direction, the anisotropy of the material can be reduced. It can be seen that the tensile strength of multilayer transparent wood is significantly higher than that of multilayer original wood, which is the common feature of the above four types of multilayer modified wood. It is further indicated that the resin PMMA and the wood template, surface layer wood, and core layer wood are well combined. To a certain extent, the toughness of wood fibers was increased by resin impregnation. Moreover, as the number of wood layers increases, the mechanical performance increases and anisotropy decreases. The above experimental results also show that different tree species can be effectively laminated through the penetration and cross-linking of the impregnated resin.

## 5. CONCLUSIONS

According to the test and calculation, the lignin of each tree species has been removed in a small amount. For Chinese fir, *B. alnoides*, and basswood, the lignin was reduced by 28.34, 30.95, and 28.29%, respectively. While retaining most of the lignin, these multilayer transparent wood samples not only have rich color and texture but also have a certain degree of light transmittance, and different kinds of tree species are used in the surface and core layers, which expands the range of raw material selection to a certain extent. It can reduce cost and energy consumption and can be prepared on demand in future production and application. Increasing the number of layers can also effectively reduce the anisotropy of thick wood. In the future, we will focus on the weather resistance of multilayer transparent wood (whether it changes differently with different times). It is hoped that such biocomposite can be used not only for indoor home decoration and structural materials but also for outdoor materials.

## AUTHOR INFORMATION


### Corresponding Author

**Yan Wu** − *College of Furnishings and Industrial Design, Nanjing Forestry University, Nanjing 210037, China; Co-Innovation Center of Efficient Processing and Utilization of Forest Resources, Nanjing Forestry University, Nanjing 210037, China;* orcid.org/0000-0003-3406-3627; Email: wuyan@njfu.edu.cn

### Authors

**Jichun Zhou** − *College of Furnishings and Industrial Design, Nanjing Forestry University, Nanjing 210037, China; Co-Innovation Center of Efficient Processing and Utilization of Forest Resources, Nanjing Forestry University, Nanjing 210037, China;* orcid.org/0000-0002-3116-9349

**Yajing Wang** − *State Key Laboratory for Modification of Chemical Fibers and Polymer Materials, Center for Advanced Low-Dimension Materials, College of Material Science and Engineering, Donghua University, Shanghai 201620, China;* orcid.org/0000-0002-6766-2549

**Jing Wang** − *College of Furnishings and Industrial Design, Nanjing Forestry University, Nanjing 210037, China; Co-Innovation Center of Efficient Processing and Utilization of Forest Resources, Nanjing Forestry University, Nanjing 210037, China*

Complete contact information is available at: https://pubs.acs.org/10.1021/acsomega.2c04842



### Funding

This work was supported by the National Natural Science Foundation of China (grant numbers 32071687 and




https://doi.org/10.1021/acsomega.2c04842
*ACS Omega* 2022, 7, 46303−46310

32001382); the Special Scientific Research Fund of Construction of High-Level Teachers Project of Beijing Institute of Fashion Technology (grant number BIFTQG201805); and the Project of Science and Technology Plan of Beijing Municipal Education Commission (grant number KM202010012001).

### Notes

The authors declare no competing financial interest.

## ■ ACKNOWLEDGMENTS

We thank the teachers of Advanced Analysis and Testing Center of Nanjing Forestry University for their help in instrument testing.

## ■ REFERENCES

(1) Li, Y.; Fu, Q.; Yu, S.; Yan, M.; Berglund, L. Optically transparent wood from a nanoporous cellulosic template: combining functional and structural performance. *Biomacromolecules* **2016**, *17*, 1358−1364.
(2) Zhu, M.; Song, J.; Li, T.; Gong, A.; Wang, Y.; Dai, J.; Yao, Y.; Luo, W.; Henderson, D.; Hu, L. Highly anisotropic, highly transparent wood composites. *Adv. Mater.* **2016**, *28*, 5181−5187.
(3) Cai, H.; Wang, Z.; Xie, D.; Zhao, P.; Sun, J.; Qin, D.; Cheng, F. Flexible transparent wood enabled by epoxy resin and ethylene glycol diglycidyl ether. *J. For. Res.* **2020**, *32*, 1779−1787.
(4) Fu, Q.; Tu, K.; Goldhahn, C.; Keplinger, T.; Adobes-Vidal, M.; Sorieul, M.; Burgert, I. Luminescent and Hydrophobic Wood Films as Optical Lighting Materials. *ACS Nano* **2020**, *14*, 13775−13783.
(5) Mi, R.; Chen, C.; Keplinger, T.; Pei, Y.; He, S.; Liu, D.; Li, J.; Dai, J.; Hitz, E.; Yang, B.; Burgert, I.; Hu, L. Scalable aesthetic transparent wood for energy efficient buildings. *Nat. Commun.* **2020**, *11*, 3836.
(6) Fu, Q.; Yan, M.; Jungstedt, E.; Yang, X.; Li, Y.; Berglund, L. Transparent plywood as a load-bearing and luminescent biocomposite. *Compos. Sci. Technol.* **2018**, *164*, 296−303.
(7) Qin, J.; Bai, T.; Shao, Y.; Zhao, X.; Li, S.; Hu, Y. Fabrication and characterization of multilayer transparent wood of different species. *J. Beijing For. Univ.* **2018**, *40*, 113−120.
(8) Foster, K. E. O.; Hess, K. M.; Miyake, G. M.; Srubar, W. V., III Optical properties and mechanical modeling of acetylated transparent wood composite laminates. *Materials* **2019**, *12*, 2256.
(9) Wu, Y.; Wang, Y.; Yang, F. Comparison of Multilayer Transparent Wood and Single Layer Transparent Wood With the Same Thickness. *Front. Mater.* **2021**, *8*, 633345.
(10) Wu, Y.; Zhou, J.; Yang, F.; Wang, Y.; Wang, J.; Zhang, J. A strong multilayered transparent wood with natural wood color and texture. *J. Mater. Sci.* **2021**, *56*, 8000−8013.
(11) Wu, S.; Xu, W. Effects of Low-Energy-Density Microwave Treatment on Graphene/Polyvinyl Alcohol-Modified Poplar Veneer. *Forests* **2022**, *13*, 210.
(12) Wu, S.; Xu, W. Sound Insulation Performance of Furfuryl Alcohol-Modified Poplar Veneer Used in Functional Plywood. *Materials* **2022**, *15*, 6187.
(13) Wu, Y.; Zhou, J.; Huang, Q.; Yang, F.; Wang, Y.; Wang, J. Study on the properties of partially transparent wood under different delignification processes. *Polymers* **2020**, *12*, 661.
(14) Wang, X.; Wu, Y.; Chen, H.; Zhou, X.; Zhang, Z.; Xu, W. Effect of Surface Carbonization on Mechanical Properties of LVL. *BioResources* **2019**, *14*, 453−463.
(15) Rao, A. N. S.; Nagarajappa, G. B.; Nair, S.; Chathoth, A. M.; Pandey, K. K. Flexible transparent wood prepared from poplar veneer and polyvinyl alcohol. *Compos. Sci. Technol.* **2019**, *182*, 107719.
(16) Huang, C.; Xu, C.; Meng, X.; Wang, L.; Zhou, X. Editorial: Isolation, Modification, and Characterization of the Constituents (Cellulose, Hemicellulose, Lignin, et al.) in Biomass and Their Bio-Based Applications. *Front. Bioeng. Biotechnol.* **2022**, *10*, 866531.
(17) Li, Y.; Fu, Q.; Rojas, R.; Yan, M.; Lawoko, M.; Berglund, L. A new perspective on transparent wood: lignin-retaining transparent wood. *ChemSusChem* **2017**, *10*, 3445−3451.
(18) Wu, J.; Wu, Y.; Yang, F.; Tang, C.; Huang, Q.; Zhang, J. Impact of delignifification on morphological, optical and mechanical properties of transparent wood. *Composites, Part A* **2019**, *117*, 324−331.
(19) Wu, Y.; Wu, J.; Wang, S.; Feng, X.; Chen, H.; Tang, Q.; Zhang, H. Measurement of mechanical properties of multilayer waterborne coatings on wood by nanoindentation. *Holzforschung* **2019**, *73*, 871−877.
(20) Liu, Y.; Zhao, G.*Wood Science*, 2nd ed.; Li, J., Ed.; China Forestry Publishing House: Beijing, 2012; pp 189−195.
(21) Lin, S.; Zhang, Q.; Ju, Y.; Duan, H. Analysis of Relationship between Chromatic Aberration Value and Pigment Content of Peel in Different Peach Varieties. *Acta Agric. Jiangxiensis* **2018**, *30*, 35.
(22) Wang, J.; Wang, Y.; Wu, Y.; Zhao, W. A Multilayer Transparent Bamboo with Good Optical Properties and UV Shielding Prepared by Diffffferent Lamination Methods. *ACS Sustainable Chem. Eng.* **2022**, *10*, 6106−6116.
(23) Xia, Q.; Chen, C.; Yao, Y.; He, S.; Wang, X.; Li, J.; Gao, J.; Gan, W.; Jiang, B.; Cui, M.; Hu, L. In Situ Lignin Modification toward Photonic Wood. *Adv. Mater.* **2021**, *33*, No. e2001588.



https://doi.org/10.1021/acsomega.2c04842
*ACS Omega* 2022, 7, 46303−46310